Surg Radiol Anat
DOI 10.1007/s00276-017-1925-9

ORIGINAL ARTICLE

Comparative anatomy on 3-D MRI of the urogenital sinus and the periurethral area before and during the second stage of labor during childbirth

Jean-Christophe Maran[1,2,3] · Lucie Cassagnes[3,4] · Vincent Delmas[2] · Dominique Musset[5] · René Frydman[6] · Gérard Mage[7] · Michel Canis[7] · Louis Boyer[3,4] · Olivier Ami[1,3,8,9]

Received: 6 July 2017 / Accepted: 13 September 2017

Abstract

Purpose of the study To describe the observable MRI changes in the urogenital sinus during the second stage of labor and delivery by comparing the changes in the positions of the anatomical structures of the maternal perineum using MRI-based vector 3-D models.

Materials and methods Seven pregnant women underwent 3-D MRI sequences using a Philips 1 T Panorama open MRI during the pre-labor period and during the second stage of labor. A 3-D vector reconstruction platform (BABYPROGRESS, France) enabled the transformation of volumes of 2-D images into finite element meshes. The polygonal meshes labeled with the principal components of the urogenital sinus were used as part of a biomechanical study of the pressure exerted on the perineum during fetal descent.

Results The expansion of the urogenital sinus was observed in all patients. Qualitative stretching was observed toward the rear and bottom of the iliococcygeus, pubococcygeus, puborectalis and obturator internus muscles. Significant length differences were measured along the iliococcygeus and pubococcygeus muscles but not along the tendinous arch of the levator ani or the puborectalis muscle. The inversion of the levator ani muscle curvature was accompanied by the transmission of pressure generated during fetal descent to the pubic muscle insertions and the descent of the tendinous arch of the levator ani.

Conclusion Mechanical pressures responsible for the tensioning of the constituent muscles of the urogenital sinus were qualitatively identified during the second stage of labor. MRI-based vector 3-D models allow the quantitative assessment of levator ani muscle stretching during labor, but 2-D MRI is not sufficient for describing perineal expansion. Vector 3-D models from larger scale studies have the potential to aid in the calibration of a realistic simulation based on the consideration of the reaction of each muscular element. These models offer perspectives to enhance our knowledge regarding perineal expansion during childbirth as a risk factor for postpartum perineal defects.

Keywords Birth imaging · Magnetic resonance imaging (MRI) · Anatomy · Urogenital sinus · Female perineum

Abbreviations

MRI	Magnetic resonance imaging
UGS	Urogenital sinus
TALA	Tendinous arch of levator ani
ICM	Iliococcygeus muscle
PCM	Pubococcygeus muscle
PRM	Puborectalis muscle

✉ Jean-Christophe Maran
jc.maran@babyprogress.fr

1 Plateforme de recherche IMAGINAITRE, Paris, France

2 Unité de Recherche en Développement, Imagerie et Anatomie (URDIA), Université Paris Descartes, EA 4465, Paris, France

3 Institut Pascal, Image Guided Therapies (IGT), UMR UCA-CNRS 6602, Aubière, France

4 CHU de Clermont Ferrand 1-Pôle de Radiologie, Clermont Ferrand, France

5 Université Paris Sud 11, Orsay, France

6 Université Paris Descartes, Paris, France

7 Service de gynécologie-obstétrique, CHU de Clermont Ferrand 1, Clermont Ferrand, France

8 Service de gynécologie-obstétrique, Clinique de l'Essonne, 2 bd des Champs Elysées, F91000 Evry, France

9 Clinique de la Muette, Ramsay Générale de Santé, Paris, France

Published online: 26 September 2017

IRB Institutional review board
ANSM French National Agency for Drug and Medical Product Safety

Introduction

The 3-D in vivo study of the maternal perineum is an essential step in the development of realistic 3-D vector models for the biomechanical study of childbirth [14, 15, 20]. These models allow a better understanding of the pressures exerted during fetal descent and their effects on the different bones, muscles, fat and visceral components of the perineum. Understanding the transmission of these pressures is an important health issue for patients and obstetricians since they are the cause of anatomic injuries that may have an impact on the pelvic floor [13, 17, 25, 27].

The biomechanical models used in contemporary simulation studies use simplistic vector sets that are not representative of the complexity of the mechanical interactions at play during childbirth [7, 14, 23, 24, 26, 28, 29]. A lack of objective knowledge of the laws of biomechanical behavior of the constituent organs of the urogenital sinus (UGS) results from the difficulty of establishing an effective imaging protocol during childbirth [6].

MRI is the only imaging modality for a complete reconstruction of the components of the birth canal during delivery, but it is dependent on fetal immobility [2, 5, 8, 12, 29]. In addition, the acquisition tunnel is often too narrow to accommodate a patient in late pregnancy [4].

The literature tends to recognize the use of ultrasonographic imaging for studying the per-partum anatomy of specific parts or organs into the pelvic floor due to the mobility and temporal resolution of this technology [14, 30, 32]. However, the thickness of the ultrasonogram's penetration power under the probe makes it difficult to visualize whole perineal soft tissue using this modality. In addition, computed tomography scanning provides poor contrast for muscles. We consider MRI a more practical modality for reconstructing perineal muscles as a whole during labor [16].

Therefore, achieving imaging during childbirth requires a machine dedicated to the large size of a woman at full term and fast acquisition sequences to minimize fetal movement artifacts. The technical requirements for completing this type of imaging also necessitate considerable organization to ensure the safety of the mother and child [1].

Following the example of Bamberg et al. in 2010 [5], who acquired dynamic 2-D MRI sequences of a birth, we obtained axial, sagittal and coronal images in an open MRI as close to term as possible before the onset of labor and in the second phase of labor, as part of normal deliveries; we also obtained dynamic sequences during pushing.

The anatomy of the UGS and its anatomical positioning before labor were compared in 3-D to its conformation in the second stage of labor, after cervical dilation, allowing fetal descent below the margin of the pelvic inlet.

The objective of this study was to describe the anatomical variations in the tendinous arch of levator ani (TALA) and the iliococcygeus (ICM), pubococcygeus (PCM) and puborectalis (PRM) muscles compared with 3-D MRI results in pregnant women before the onset of labor and during the second stage of labor and perineal extension.

Materials and methods

Twenty-seven pregnant women were examined with 3-D MRI sequences before going into labor; seven of them underwent follow-up 3-D MRI imaging during the second phase of labor in a 1 T open MRI (Panorama, Philips UK) as part of a French biomedical study (IMAGINAITRE, BirthXplore). This prospective research protocol was approved by the "Ile de France II" institutional review board (IRB) and by the French National Agency for Drug and Medical Product Safety (ANSM) and was promoted by the University of Clermont-Ferrand Medical Center. The imaging was performed at the Essonne Clinic, which combines a maternity ward and an MRI radiology department in the same building.

Clinical protocol

The inclusion criteria for the study included pregnant women; aged 21–39 years; primipara, secundipara or tertipara; with no known factors that could affect delivery; who agreed to participate and signed an informed consent form.

Exclusion criteria for the study included fetal breech presentation or not strictly cephalic at the time of delivery, scarred uterus, multiple pregnancy, known maternal or fetal medical conditions requiring urgent care, abnormal fetal heart rate requiring treatment within half an hour, contraindication to MRI imaging, a minor or incompetent adult patient, and no prior obstetrical care during pregnancy.

MRI scans were performed on all 27 included patients during the final 4 days of their pregnancy and before the onset of labor. The imaging was repeated in seven cases during the second phase of labor, immediately before the start of the expulsive effort. Entry into the second phase of labor was marked by complete cervical dilation accompanied by the drop of the fetal head and its engagement between the superior pelvic strait and the middle of the pelvic brim, as verified by clinical examination.

The protocol included the completion of an MRI scan in the dorsal decubitus position before labor and in the same position during the second stage of labor, along with sequences during a change in maternal position (from dorsal

decubitus to lateral decubitus) to determine any changes in the rotation and trajectory of the fetal head. Only the results of the MRI in the dorsal decubitus position before and during the second stage of labor are reported in this study.

Safety

A double clinical team, available 24 h per day, was put in place for this protocol, and technical provisions for maternity and radiology were made available to the IMAGINAITRE research platform with sufficient staff to ensure patient safety. The location of an open MRI in the same building as the delivery room was decisive in the choice of site to implement this protocol in France.

The transportation time of patients between the MRI and delivery room did not exceed 3 min (from bed to bed). At all times, the parturients had the same monitoring and safety conditions as in the delivery room. The time during which the fetal heart rate was not recorded during the entire protocol did not exceed ten cumulative minutes.

Imaging protocol

The same protocol was used for tests before and during the second stage of labor, with the same sequences, the same antennas and the same conditions of implementation in terms of maternal position.

The sequences used were fast and contiguous sequences. The protocol included a localization sequence; acquisition of contiguous frontal, sagittal and axial T1-weighted, 3-D gradient echo; and a T2-weighted acquisition of fetal brain volume and a 1-min dynamic acquisition sagittally centered on the birth canal.

The MRI conditions were as follows: 3-D T1-FFE (E-Thrive—Philips, UK) single-shot sequence without FAT-SAT; TE = 1.62 ms; TR = 3.2 ms; matrix = 448 × 448 pixels; angle = 10; TFE factor 82; NSA; 160 overlapping sections; acquisition voxel size = 2.2 mm; and reconstructed voxel size = 1 mm.

To facilitate comparisons, the resetting of the imaging and 3-D reconstructions was performed on fixed points of the maternal pelvis (acetabulum, pubis, iliac crests, the promontory of the sacrum, and the coccyx).

The imaging was performed in an open 1-T Philips PANORAMA MRI located in the same building as the maternity ward.

The height reached by the presentation between the imaging performed before labor and that during labor was evaluated according to midline imaging criteria proposed by DIETZ et al. [9] and correlated to MRI by Güttler et al. [12]. The measurement method consisted of defining a perpendicular reference to the major axis of the symphysis pubis in the sagittal plane through the lower edge of the pubis, measuring the height of the descent of the lowest point of the fetal head compared to the said line, and measuring the difference in the height between before the onset of labor and in the second stage of labor. The angle of progression formed by these reference points and observed at these two stages of labor was also measured.

Post-processing of 3-D imaging

We used a SIMULACC™ (Baby Progress SAS—Paris—France) workstation equipped with PREDIBIRTH™ software (Olivier Ami, MD) to perform 3-D vector reconstructions. Vectorization of the contours was computer aided, and the results were supervised by obstetricians and radiologists. Two-dimensional slice-based comparative measurements of the levator hiatus dimensions (the levator hiatal area and the anteroposterior and transverse diameters) were assessed on MRI image stacks as described by Vergeldt et al. in 2011 [32]. As recommended by Hoyte et al. in 2009 [14], 3-D reconstruction-based measurements, with well-defined anatomical landmark edges, were performed on the levator ani muscles and were compared during and before labor. TALA, ICM, PCM and PRM were assessed lengthwise. Transverse diameters were not retained due to insufficient knowledge regarding intraperineal muscular landmarks during perineal swelling.

Statistical analysis

To characterize the anatomical changes observed in the small sample of patients in this study, Wilcoxon's signed-rank test was performed to test the null hypothesis of a significant difference between measurements before and during the second stage of labor. The test was chosen considering the small size of the sample in this study and the lack of knowledge of the distribution of quantitative variables. The anatomical changes are described as significantly related to the second stage of labor ($p < 0.05$). Correlations between quantitative measures were assessed using both Pearson and Spearman coefficients.

Results

Population

Out of 27 volunteers who agreed to participate in this protocol, seven gave birth under conditions that allowed for an exploitable MRI during the second phase of labor (Table 1). The seven patients included were 28 years old on average (range 23–34 years), three were primipara, three were secundipara, and one was tertipara. All were beyond 39 weeks of gestation, and four of them were past their due date.

Table 1 Characteristics of the seven patients on whom we were able to perform an MRI in the second phase of labor

Patients	Age	Parity	Term in SA	MAGNIN	Fetal weight in g	Height in cm	Perineum	Delivery type	Descent delta according to DIETZ in mm	Angle delta according to DIETZ in degrees
Patient 1	23	1	40	25.1	3380	51	Intact	Normal	27.37	21.6
Patient 2	28	2	41	26.7	4000	53	Scuffing	Normal	23.07	17.6
Patient 3	28	1	41	26.1	3755	55	Intact	C-section at full dilatation	31.15	26.5
Patient 4	31	2	41	25.1	4525	54	Single tear	Normal	53.79	48.5
Patient 5	31	2	39	27.5	3095	49	Intact	Normal	30.56	24.2
Patient 6	34	3	39	27.1	4145	52	Single tear	Normal	29.91	26.1
Patient 7	24	1	41	25.6	3625	51	Intact	C-section at full dilatation failed forceps	25.54	25.3
Median	28	2	41	26.1	3755	52	4 intact	2 c-sections	29.91	25.3

The drop of the fetal head was evaluated according to the method of DIETZ et al. in sagittal section with a distance of descent calculated at the lowest point of the fetal head compared to the perpendicular axis at the lower edge of the mother's pubic bone, and at the angle formed between this axis and the straight line passing through the lower edge of the mother's pubic bone and the lowest point of the fetal head. The differences between descent and angle before and during second stage of labor, according to Dietz, are reported in this table

The median Magnin score of the participants was 26 (25.1–27.5). The newborns had a median weight of 3755 g (3095–4525 g).

Five children were born by natural delivery without instrumental extraction, and two were born by emergency cesarean section due to stagnation when fully dilated—one after forceps failure. In both cases, the pregnancies were overdue.

No patient had dystocia predictable from the size of the pelvis since all Magnin scores were above 25.

All participating patients were fully dilated, and their fetuses descended a median of 29.9 mm and at a 25.3° angle according to the measuring method of Dietz et al.

Anatomic changes in UGS

The descent of the fetal head causes an expansion of the UGS, which is better demonstrated with 3-D finite elements reconstruction, from the contact of the fetal head with the ICM of the levator ani muscles (Fig. 1). Comparative measurements are difficult on 2-D MRI slices due to the important anatomical changes observed during labor (Fig. 2). Taking into account the complexity of correlating muscular visual landmarks during labor, those distances were not measured in this study.

An inversion of the levator ani muscle's curvature was observed in all cases, regardless of the fetal head descent level. The forward and downward thrusts exerted pressure, notably on the pubic insertions of the PRM and the lateral insertions of the ICM of the levator ani. This pressure was exerted laterally on the thickenings of the fascia of the obturator internus muscle forming the TALA and throughout the pelvic fascia, which was tensioned upward through the tendinous arch of pelvic fascia (Figs. 1, 3).

The TALA, on which the levator ani muscles lie, was pushed downward and sideways but remained statistically significantly conserved in length (Wilcoxon signed-rank test, $p < 0.05$) (Fig. 3) (Table 2). Pubic insertions of the PRM were stretched and flattened along the internal surface of the pubis, as demonstrated in the 3-D reconstruction (Fig. 1). The PRM length did not demonstrate significant elongation during labor (Wilcoxon signed-rank test, $p < 0.05$).

The anterior fascial insertions of the ICM on the obturator internus muscles were pushed sideways and downward, and the verticalization of the ICM was better observed in the frontal view with a higher lift on the anterior part of the muscles. The Wilcoxon signed-rank test yielded significant differences between before labor and during labor acquisitions for the ICM and PCM lengths ($p < 0.05$).

A statistical asymmetry was measured between the left and right ICMs during labor (Wilcoxon signed-rank test, $p < 0.05$). The right ICM was 8.1 mm longer on average than the left ICM during the second stage of labor. It was

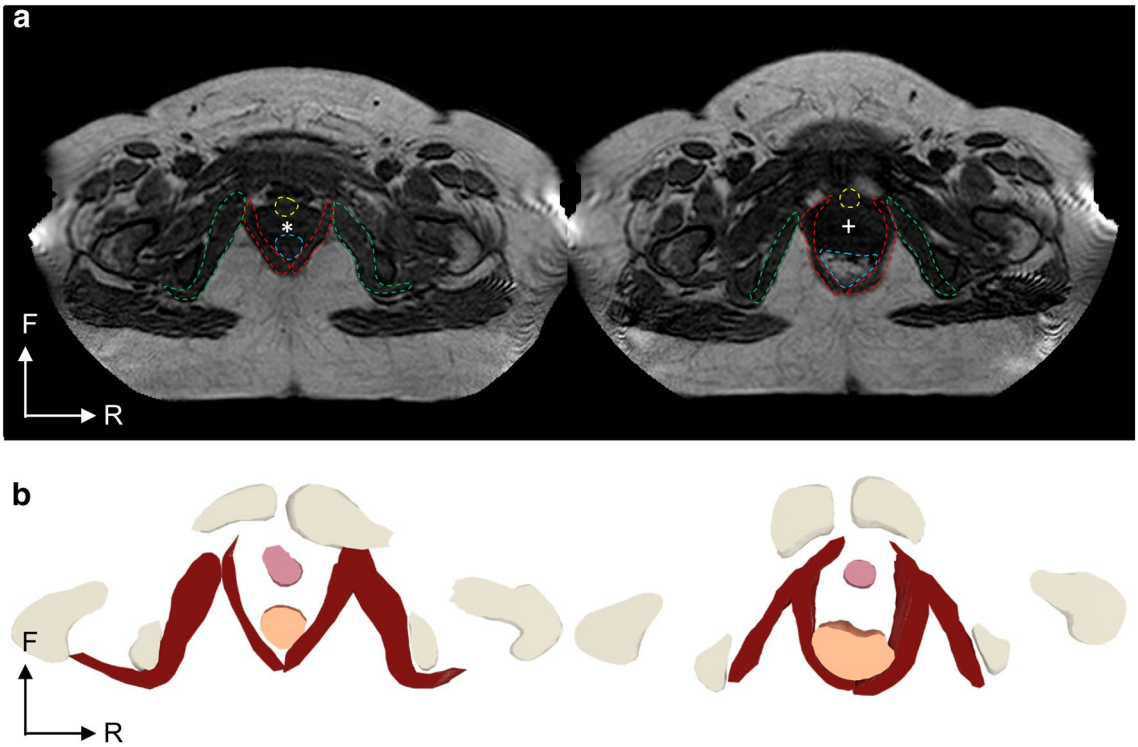

Fig. 1 **a** MRI axial slices of the UGS before (left) and during (right) the second stage of labor. The urethra (yellow dashed line) is brought forward during the descent of the fetal head (+) through the vagina (*). The vagina is no longer visible during the expansion of the perineum. The anterior fascial insertions of iliococcygeal muscles (red dashed lines) on obturator internus muscles (green dashed lines) are pushed sideways. Obturator internus muscles are thickening, principally along their anterior portion. The rectum (¤) is pushed backward and flattened against the internal surface of the levator ani muscles. We can observe a ballooning of the iliococcygeal muscles and an enlargement of the UGS during the fetal head descent. **b** Superior view of axial sliced 3D reconstructions of the structures highlighted on the MRI slices (vagina and fetal head excepted), before (left) and during (right) the second stage of labor. Anatomical changes depicted in 2D are visible on muscles (red), urethra (pink) and rectum (brown). The expansion of the UGS is clearly visible

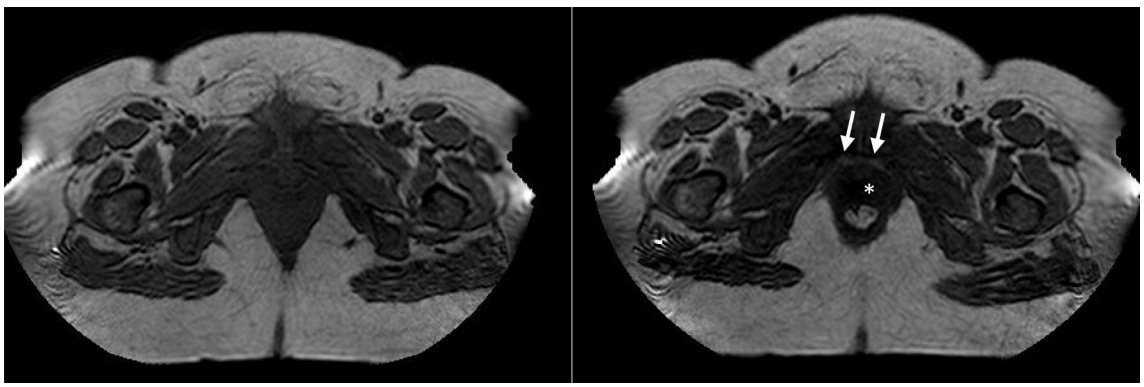

Fig. 2 Highlighting anatomical visual changes on a single matching slice between the two times of acquisition. The perineal plane visible on the left slice is more superficial than the one visible during labor on the right slice. We can see retropubic fat insinuation (arrows) and the caput succedaneum (*) during the second stage of labor

not possible to establish a clear correlation between the fetal head orientation and any major changes or asymmetry observed in this small series. A moderate positive correlation was calculated between the delta Dietz level of descent and PRM stretching, with Pearson and Spearman coefficients of 0.576 ($p = 0.05$) and 0.595 ($p = 0.041$), respectively. This result suggests that within the fetal descent Dietz criterion margin observed during the study (i.e., a descent between

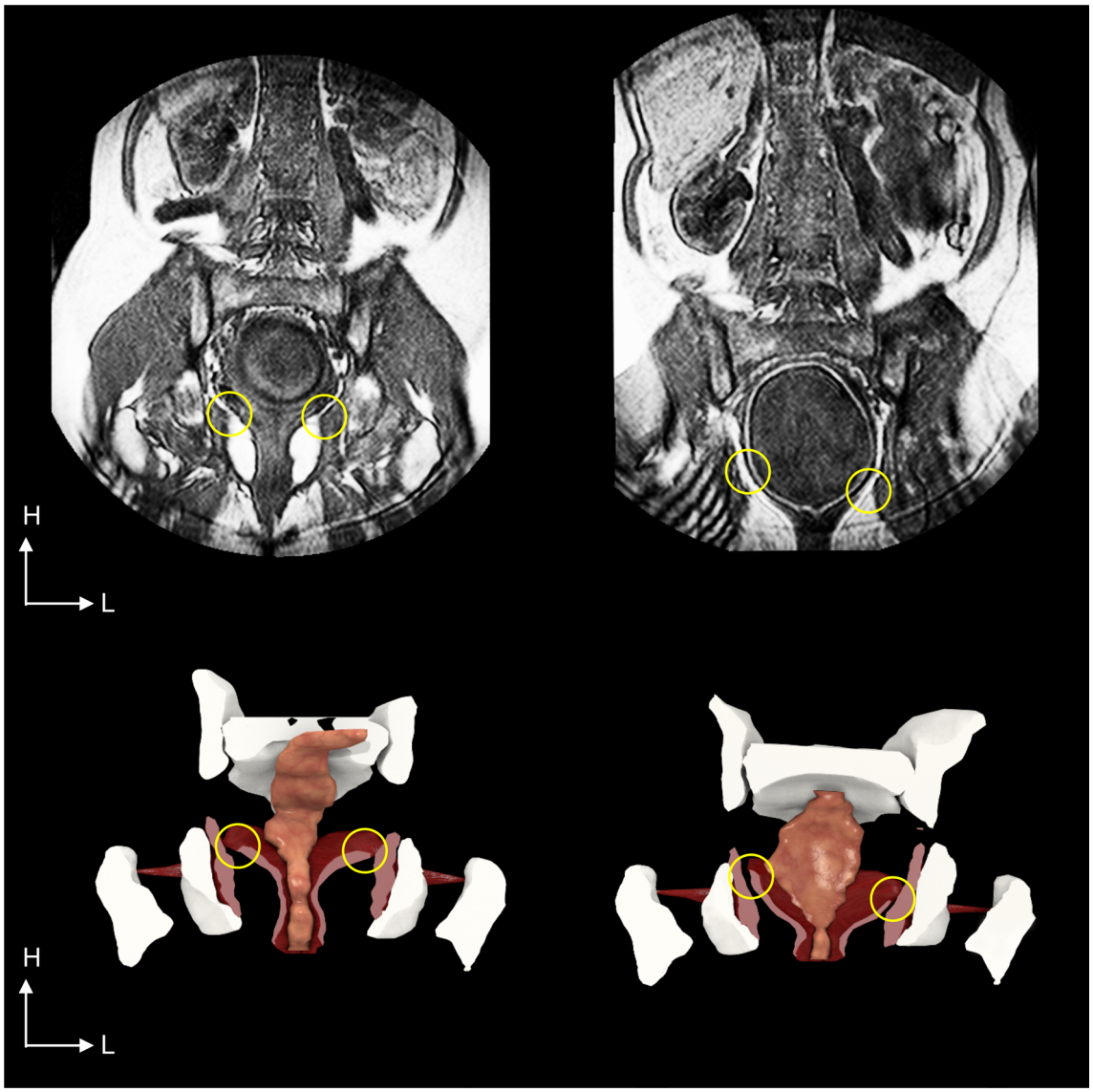

Fig. 3 Imaging of the inversion of the levator ani's curvature on frontal MRI slices (up) and their 3D reconstructions (down) before (left) and during (right) the second stage of labor. Major musculoskeletal structures, such as obturator internus muscles and levator ani muscles, are 3D meshed. The fetal head descends through the perineum; this flattens the rectum (brown colored mesh) against both the sacrum and posterior internal surface of the levator ani muscles. TALAs (yellow circles) are visibly pushed down and sideways during the second stage of labor

2.3 and 5.3 cm according to Dietz), the PRM exhibited a low linear deformation, depending on the engagement of the fetal head.

The urethra was pushed forward during the expansion of the perineum for the descent of the fetal head, pushing the retropubic fat down under the lower margin of the pubis (Fig. 2). In the sagittal view, urethral compression by the fetal head resting against the pubic symphysis was visible in the second stage of labor when the bladder transitioned to the suprapubic position (six cases out of seven). In semi-repletion, the bladder appeared to be stretched lengthwise and taut between the urachus and pubis. In cases in which the bladder was empty, it remained under and behind the pubis, maintaining its flexible path. The urethra was brought down and pulled by the fetal head under the lower margin of the pubis (one case out of seven) (Fig. 4).

Discussion

The 3-D meshes reconstructed from MRI allowed us to better visualize and understand the anatomical changes in the UGS during the second phase of labor. Some measurements difficult to perform in 2-D imaging were demonstrated to

Table 2 On the left, 3-D-based measurements of different parts of both right and left levator ani muscles of six patients included in the study, before and during the second stage of labor

Patients	Right Before	Right During	Left Before	Left During	Fetal presentation
TALA_1	69	71	72,4	73,3	LOA
TALA_2	81,8	78,8	74,1	66,7	ROT
TALA_3	86,6	88,2	98,27	86	LOA
TALA_4	80,7	82	75,2	73,52	LOA
TALA_6	54,6	42	60,7	47,7	ROP
TALA_7	64,9	61,3	70,9	63,6	LOA
ICM_1	83,8	90,6	84,4	81,3	LOA
ICM_2	94,7	104,1	95,8	94,6	ROT
ICM_3	76	95,4	60,1	92,9	LOA
ICM_4	88,1	112,1	81,1	94,6	LOA
ICM_6	70,7	72,9	72,5	67,9	ROP
ICM_7	60,8	79,3	67,5	74,3	LOA
PCM_1	98,2	107,7	89,1	94,8	LOA
PCM_2	103,8	136	116,1	122,4	ROT
PCM_3	102,1	111,6	99,9	125,9	LOA
PCM_4	93,2	122,7	102,8	108,87	LOA
PCM_6	93,8	89,9	85,9	99,7	ROP
PCM_7	71,9	85,6	71,2	79,9	LOA
PRM_1	80,5	89,7	70,3	82,37	LOA
PRM_2	78	79,6	79,1	66	ROT
PRM_3	83,7	93,2	90,7	107,9	LOA
PRM_4	70,5	102,3	74,1	81,7	LOA
PRM_6	80,1	70,5	79,5	69,9	ROP
PRM_7	64,8	67	60,2	65,1	LOA

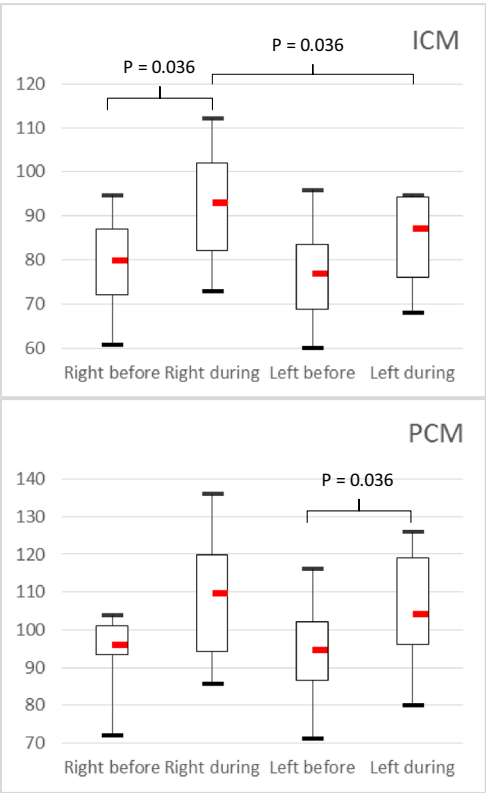

Patient 5, with intact membranes, has been excluded from these results. Parts identification was based on anatomical landmarks such as the coccyx, the pubic ramus and the TALA and validated by a radiologist. On the right, box plots data from ICM and PCM, which present significant differences in length between both times of acquisition. An asymmetry is highlighted during labor for ICM. Presentations are: *LOA* left occiput anterior, *ROT* right occiput transverse, *ROP* right occiput posterior

be feasible in 3-D despite the perineal anatomical changes endured during labor.

Urinary incontinence is usually due to hypermobility of the urethrovesical junction and is associated with grand multiparity and a history of delivering large infants [13, 22]. Imaging during the second stage of labor allowed the observation of the biomechanical pressures affecting the anatomical structures immediately surrounding the urethra.

The urethra was heavily used in the flaring of the UGS, being compressed against the symphysis pubis (Figs. 1, 4). The bladder was observed in semi-repletion in six of seven cases, forcing the urethra to stretch vertically. This configuration seemed to make it less likely to be pulled down by the fetal head, which could affect the integrity of the joints of the urethrovesical junction.

However, stretching the UGS area leads to a refinement of the pubic insertions of the levator ani along the posterior surface of the pubis. During childbirth, the urethra is in direct contact with the fetal head during its descent into the birth canal. The horizontal thrusts affecting the UGS come from the center of the pelvic cavity, and the vertical thrusts exert a downward force. The female urethra has retropubic and lateral joints, but in the case of bladder sphincter lowering, it can be located between the pubis and the fetal head at the time of its descent, suggesting that a wrenching of urethral suspension may occur.

The musculotendinous structures of the periurethral area play an important role in pelvic equilibrium, avoiding the descent of the urethrovesical junction below the margin of the pubis, which might prevent urinary incontinence [33–35]. This support system undergoes significant geometric changes during the passage of the fetus through the birth canal [31]. These deformations, although not quantified, allowed the orientation of the forces applied to the UGS's muscular insertions to be observed by comparing the movements of anatomical structures successively at different points in the delivery.

In its participation in perineal expansion during childbirth, the support system of the urethra and bladder does not seem to be limited to muscle insertions from the PRM of the levator ani; instead, it seems to involve more distant structures that are complex and act sequentially.

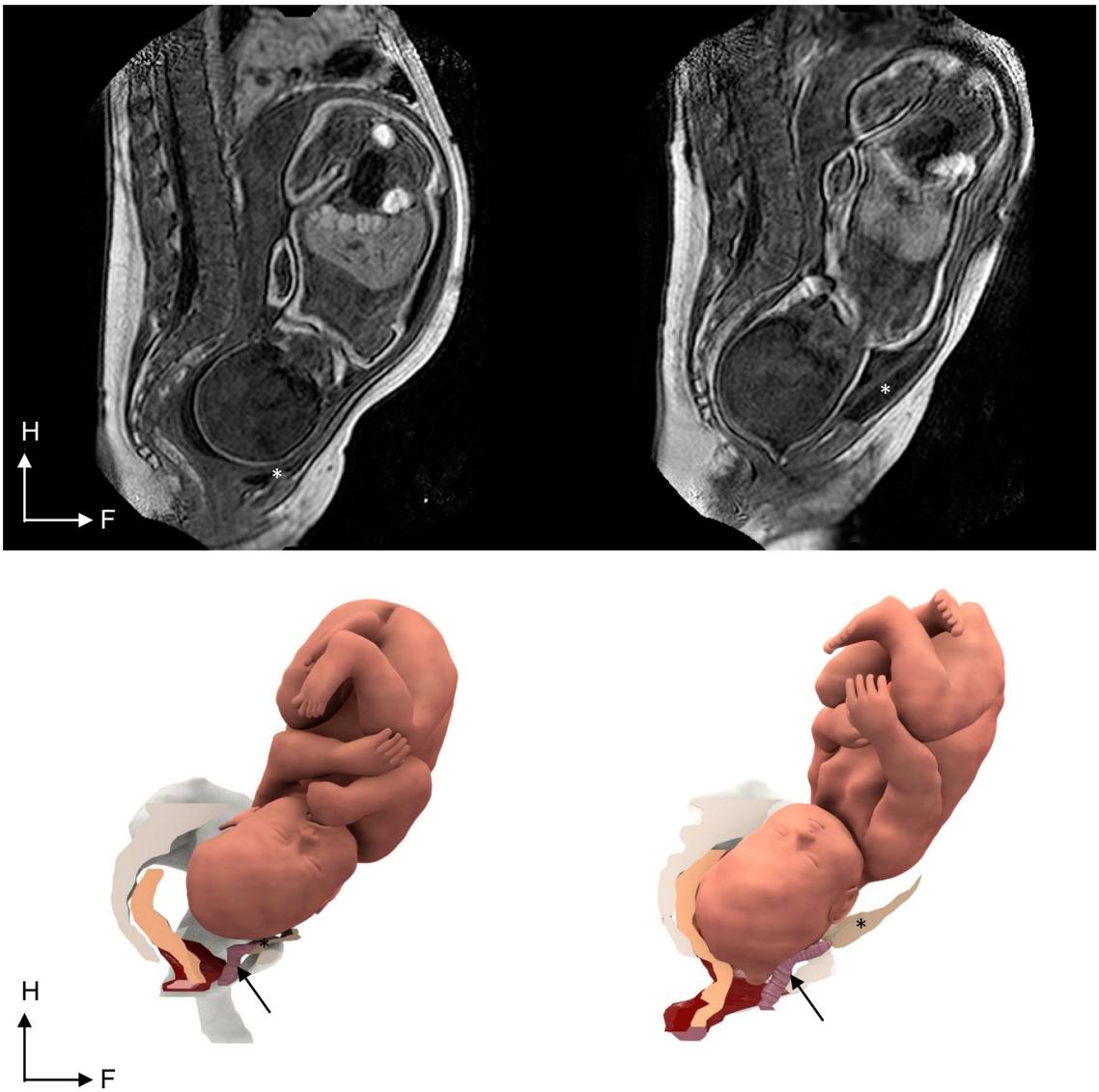

Fig. 4 Imaging of the bladder before (left) and during (right) the second phase of labor, in MRI slices (up) and 3D (down). Before labor, the bladder is located between the fetal head and the pubis. The fetal head's descent causes the bladder, in semi-repletion at that point, to move upward into a suprapubic position. Simultaneously the urethra is lifted (arrow) and pushed against the internal surface of the pubis

The biomechanical role of the visible periurethral fat spaces observed using imaging has been studied minimally or not at all. However, these spaces have sliding surfaces whose consistencies are highly dependent on the local temperature.

Similarly, the mobility of the fascial systems is rarely observed in dynamic imaging. Childbirth MRI exploration could help elucidate this complex tendinous system; nevertheless, the imaging performed sequentially during the birthing process allowed us to observe that the various musculofascial structures of the pelvic cavity were sequentially mobilized during the passage of the fetal head. The verticalization of the ICM caused the lowering of the PRM and pulled the TALA and pelvic fascia laterally and downward. The pelvic fascia was in turn tensioned, and these changes all minimized the hindrance of the organs in the pelvic cavity to allow the passage of the fetal head.

The ICM and PCM were significantly stretched by the descent of the fetal head in the presented results, according to Wilcoxon's signed-rank test, revealing the pliability of these deep parts of the levator ani.

On the one hand, these findings suggest that the TALA is strongly stretch resistant. The TALA provides key support for surrounding structures, such as the arcus tendineus fascia pelvis and the vaginal wall. These structures are often involved in paravaginal defects [3] and cystocele [11]. The resistance of the TALA to stretching is consistent with a protective role during perineal expansion.

On the other hand, it seems that the PRM is subjected to a late mechanical load compared with the ICM and PCM. The ICM and PCM did not show any reliable correlation with Dietz level difference. Although the perineal descent consecutive to the inversion of the levator ani muscle curvature began as soon as the fetal head came into contact with the muscles, the elongation of the PRM required a further stage in the descent. The PRM, in the earliest stage of labor, seems to exhibit a linear positive correlation with the fetal head descent level.

These findings suggest that perineal soft tissues, particularly levator ani deep components, are a direct reflection of the presentation asymmetry of the fetus and that they play important roles in the biomechanics of fetal descent. Their mechanical behavior during childbirth appears to be complex, and their exploration may lead to reconsiderations of the biomechanical models applied to date, such as Oliveira's [26], and improvements of their solutions with data implemented from delivery imaging.

This study is limited by the number of observed cases due to the complexities involved in organizing an MRI research protocol during childbirth. However, the statistical results obtained in this work may form a basis for the exploitation of MRI for childbirth exploration. The data extracted in this study contribute to the definition of accurate deformation models for better simulations.

The literature contains empirical data on the surface anatomy of perineal extension or cadaver anatomical observations, transperineal and transvaginal ultrasound studies [9, 10] that do not show all of the pelvic anatomical landmarks, or 3-D simulations from theoretical models with drawings [14, 18, 19, 21, 26].

The muscular changes visible on 2-D MRI are difficult to assess due to the lack of knowledge about potential anatomical landmarks during fetal head descent. The swelling of the periurethral hiatus, led by the stretching of the PCM toward the pelvic outlet, requires more than 2-D slices for proper evaluation. Many of the changes observed during this study were previously known but have never been demonstrated by direct 3-D MRI imaging during childbirth. These findings yield a more realistic 3-D reconstruction of the anatomical changes during the second stage of labor.

Anatomical landmarks observed with 3-D MRI allow for better estimation of the relationships between the levator ani and the internal obturator muscles as well as better observations of the reactions of all layers from the deep to superficial perineum during the fetal head descent, which are impossible in 2-D. This study demonstrates the potential of MRI-based 3-D vector reconstruction for defining relevant measurements for the evaluation of perineal changes.

The perspectives offered by this work include improved mathematical modeling of normal childbirth from 3-D functional anatomy observations, as suggested by Bamberg et al. [4]. The data resulting from this work could provide information about perineal changes during childbirth. In particular, bony diameters, whose landmarks remain well defined during labor, could improve our comprehension of childbirth biomechanics, combining the strengths of both 2-D- and 3-D-based measurements. The knowledge enhancement expected from a larger scale study should be considered in future implementations for a more accurate computed simulation model of perineal extension during labor.

Conclusion

The TALA is a central node of tension and did not show any significant changes during the descent of the fetal head, which supports the hypothesis of its protective role.

The ICM and PCM seemed responsive to the mechanical solicitation triggered by the fetal head descent. Significant asymmetry was measured during fetal head descent on the ICM and PCM, which indicates significant stretching during labor. No correlation was established between presentation and the ICM asymmetry measured in this series. The PRM was subject to fetal head descent-related deformation late in labor.

The bladder being in semi-repletion seems to be protective for the urethrovesical junction from a biomechanical point of view.

These results provide a better understanding of the biomechanical phenomena and forces acting upon the maternal perineum during childbirth.

Compliance with ethical standards

Conflict of interest The authors declare that they have no conflicts of interest to disclose.

Ethical approval All procedures performed in studies involving human participants were in accordance with the ethical standards of the institutional and/or national research committee and with the 1964 Helsinki declaration and its later amendments or comparable ethical standards.

Informed consent Informed consent was obtained from all individual participants included in the study.

References

1. Ami O, Chabrot P, Jardon K, Rocas D, Delmas V, Boyer L, Mage G (2011) Detection of cephalopelvic disproportion using a virtual reality model: a feasibility study of three cases. J Radiol 92:40–45. doi:10.1016/j.jradio.2009.05.001
2. Ami O, Chabrot P, Rabischong B, Rocas D, Delmas V, Boyer L, Mage G (2010) Tridimensional vector animation from fetal MRI as a simulation of delivery. J Radiol 91:515–517

3. Arenholt LTS, Pedersen BG, Glavind K, Glavind-Kristensen M, DeLancey JOL (2016) Paravaginal defect: anatomy, clinical findings, and imaging. Int Urogynecol J. doi:10.1007/s00192-016-3096-3
4. Bamberg C, Deprest J, Sindhwani N, Teichgräberg U, Güttler F, Dudenhausen JW, Kalache KD, Henrich W (2016) Evaluating fetal head dimension changes during labor using open magnetic resonance imaging. J Perinat Med. doi:10.1515/jpm-2016-0005
5. Bamberg C, Rademacher G, Güttler F, Teichgräber U, Cremer M, Bührer C, Spies C, Hinkson L, Henrich W, Kalache KD, Dudenhausen JW (2012) Human birth observed in real-time open magnetic resonance imaging. Am J Obstet Gynecol 206:505.e1–505.e6. doi:10.1016/j.ajog.2012.01.011
6. Buttin R, Zara F, Shariat B, Redarce T, Grangé G (2013) Biomechanical simulation of the fetal descent without imposed theoretical trajectory. Comput Methods Programs Biomed 111:389–401. doi:10.1016/j.cmpb.2013.04.005
7. Cosson M, Rubod C, Vallet A, Witz J-F, Brieu M (2011) Biomechanical modeling of pelvic organ mobility: towards personalized medicine. Bull Acad Natl Méd 195:1869–1883 **(discussion 1883)**
8. Delmas V, Ami O, Iba-Zizen M-T (2010) Dynamic study of the female levator ani muscle using MRI 3D vectorial modeling. Bull Acad Natl Méd 194:969–980 **(discussion 981–982)**
9. Dietz HP, Lanzarone V (2005) Measuring engagement of the fetal head: validity and reproducibility of a new ultrasound technique. Ultrasound Obstet Gynecol Off J Int Soc Ultrasound Obstet Gynecol 25:165–168. doi:10.1002/uog.1765
10. Dietz HP, Shek KL (2009) Levator defects can be detected by 2D translabial ultrasound. Int Urogynecol J Pelvic Floor Dysfunct 20:807–811. doi:10.1007/s00192-009-0839-4
11. Eisenberg VH, Chantarasorn V, Shek KL, Dietz HP (2010) Does levator ani injury affect cystocele type? Ultrasound Obstet Gynecol Off J Int Soc Ultrasound Obstet Gynecol 36:618–623. doi:10.1002/uog.7712
12. Güttler FV, Heinrich A, Rump J, de Bucourt M, Schnackenburg B, Bamberg C, Hamm B, Teichgräber UK (2012) Magnetic resonance imaging of the active second stage of labour: proof of principle. Eur Radiol 22:2020–2026. doi:10.1007/s00330-012-2455-9
13. Howard D, Makhlouf M (2016) Can pelvic floor dysfunction after vaginal birth be prevented? Int Urogynecol J. doi:10.1007/s00192-016-3117-2
14. Hoyte L, Brubaker L, Fielding JR, Lockhart ME, Heilbrun ME, Salomon CG, Ye W, Brown MB, Pelvic Floor Disorders Network (2009) Measurements from image-based three dimensional pelvic floor reconstruction: a study of inter- and intraobserver reliability. J Magn Reson Imaging JMRI 30:344–350. doi:10.1002/jmri.21847
15. Hoyte L, Damaser MS (2007) Magnetic resonance-based female pelvic anatomy as relevant for maternal childbirth injury simulations. Ann N Y Acad Sci 1101:361–376. doi:10.1196/annals.1389.018
16. Hoyte L, Ye W, Brubaker L, Fielding JR, Lockhart ME, Heilbrun ME, Brown MB, Warfield SK, Pelvic Floor Disorders Network (2011) Segmentations of MRI images of the female pelvic floor: a study of inter- and intra-reader reliability. J Magn Reson Imaging JMRI 33:684–691. doi:10.1002/jmri.22478
17. Lamblin G, Mayeur O, Giraudet G, Jean Dit Gautier E, Chene G, Brieu M, Rubod C, Cosson M (2016) Pathophysiological aspects of cystocele with a 3D finite elements model. Arch Gynecol Obstet. doi:10.1007/s00404-016-4150-6
18. Lapeer R, Audinis V, Gerikhanov Z, Dupuis O (2014) A computer-based simulation of obstetric forceps placement. Med Image Comput Comput-Assist Interv MICCAI Int Conf Med Image Comput Comput-Assist Interv 17:57–64
19. Lee S-L, Tan E, Khullar V, Gedroyc W, Darzi A, Yang G-Z (2009) Physical-based statistical shape modeling of the levator ani. IEEE Trans Med Imaging 28:926–936. doi:10.1109/TMI.2009.2012894
20. Lepage J, Cosson M, Mayeur O, Brieu M, Rubod C (2016) The role of childbirth research simulators in clinical practice. Int J Gynaecol Obstet Off Organ Int Fed Gynaecol Obstet 132:234–235. doi:10.1016/j.ijgo.2015.07.017
21. Lepage J, Jayyosi C, Lecomte-Grosbras P, Brieu M, Duriez C, Cosson M, Rubod C (2015) Biomechanical pregnant pelvic system model and numerical simulation of childbirth: impact of delivery on the uterosacral ligaments, preliminary results. Int Urogynecol J 26:497–504. doi:10.1007/s00192-014-2498-3
22. da Leroy L, Lúcio A, de Lopes MHBM (2016) Risk factors for postpartum urinary incontinence. Rev Esc Enferm UP 50:200–207. doi:10.1590/S0080-623420160000200004
23. Lien K-C, Morgan DM, Delancey JOL, Ashton-Miller JA (2005) Pudendal nerve stretch during vaginal birth: a 3D computer simulation. Am J Obstet Gynecol 192:1669–1676. doi:10.1016/j.ajog.2005.01.032
24. Li X, Kruger JA, Nash MP, Nielsen PMF (2010) Effects of nonlinear muscle elasticity on pelvic floor mechanics during vaginal childbirth. J Biomech Eng 132:111010. doi:10.1115/1.4002558
25. Miller JM, Low LK, Zielinski R, Smith AR, DeLancey JOL, Brandon C (2015) Evaluating maternal recovery from labor and delivery: bone and levator ani injuries. Am J Obstet Gynecol 213:188.e1–188.e11. doi:10.1016/j.ajog.2015.05.001
26. Oliveira DA, Parente MPL, Calvo B, Mascarenhas T, Natal Jorge RM (2016) Numerical simulation of the damage evolution in the pelvic floor muscles during childbirth. J Biomech 49:594–601. doi:10.1016/j.jbiomech.2016.01.014
27. Shi M, Shang S, Xie B, Wang J, Hu B, Sun X, Wu J, Hong N (2016) MRI changes of pelvic floor and pubic bone observed in primiparous women after childbirth by normal vaginal delivery. Arch Gynecol Obstet 294:285–289. doi:10.1007/s00404-016-4023-z
28. Silva MET, Oliveira DA, Roza TH, Brandão S, Parente MPL, Mascarenhas T, Natal Jorge RM (2015) Study on the influence of the fetus head molding on the biomechanical behavior of the pelvic floor muscles, during vaginal delivery. J Biomech 48:1600–1605. doi:10.1016/j.jbiomech.2015.02.032
29. Tracy PV, DeLancey JO, Ashton-Miller JA (2016) A geometric capacity-demand analysis of maternal levator muscle stretch required for vaginal delivery. J Biomech Eng 138:021001. doi:10.1115/1.4032424
30. Unger CA, Weinstein MM, Pretorius DH (2011) Pelvic floor imaging. Obstet Gynecol Clin North Am 38:23–43. doi:10.1016/j.ogc.2011.02.002
31. van Veelen A, Schweitzer K, van der Vaart H (2014) Ultrasound assessment of urethral support in women with stress urinary incontinence during and after first pregnancy. Obstet Gynecol 124:249–256. doi:10.1097/AOG.0000000000000355
32. Vergeldt TFM, Notten KJB, Stoker J, Fütterer JJ, Beets-Tan RG, Vliegen RFA, Schweitzer KJ, Mulder FEM, van Kuijk SMJ, Roovers JPWR, Kluivers KB, Weemhoff M (2016) Comparison of translabial three-dimensional ultrasound with magnetic resonance imaging for measurement of levator hiatal biometry at rest. Ultrasound Obstet Gynecol Off J Int Soc Ultrasound Obstet Gynecol 47:636–641. doi:10.1002/uog.14949
33. Wijma J, Weis Potters AE, van der Mark TW, Tinga DJ, Aarnoudse JG (2007) Displacement and recovery of the vesical neck position during pregnancy and after childbirth. Neurourol Urodyn 26:372–376. doi:10.1002/nau.20354
34. Zacharin RF (1968) The anatomic supports of the female urethra. Obstet Gynecol 32:754–759
35. Zacharin RF (1977) Abdominoperineal urethral suspension: a 10-year experience in the management of recurrent stress incontinence of urine. Obstet Gynecol 50:1–8